

LETTER • **OPEN ACCESS**

Mechanisms of the decadal variability of monsoon rainfall in the southern Tibetan Plateau

To cite this article: Siyu Yue *et al* 2021 *Environ. Res. Lett.* **16** 014011

View the [article online](#) for updates and enhancements.

ENVIRONMENTAL RESEARCH
LETTERS

LETTER

OPEN ACCESS

RECEIVED
2 May 2020REVISED
27 October 2020ACCEPTED FOR PUBLICATION
17 November 2020PUBLISHED
21 December 2020

Original content from
this work may be used
under the terms of the
[Creative Commons
Attribution 4.0 licence](#).

Any further distribution
of this work must
maintain attribution to
the author(s) and the title
of the work, journal
citation and DOI.



Mechanisms of the decadal variability of monsoon rainfall in the southern Tibetan Plateau

Siyu Yue¹ , Bin Wang^{2,3}, Kun Yang^{1,4} , Zhiling Xie^{2,3} , Hui Lu¹ and Jie He¹¹ Ministry of Education Key Laboratory for Earth System Modeling, Department of Earth System Science, Tsinghua University, Beijing 10084, People's Republic of China² International Pacific Research Center, School of Ocean and Earth Science and Technology, University of Hawaii at Manoa, Honolulu, HI 96825, United States of America³ Earth System Modeling Center, Nanjing University of Information Science and Technology, Nanjing 210044, People's Republic of China⁴ CETES, Institute of Tibetan Plateau Research, Chinese Academy of Sciences, Beijing 100101, People's Republic of ChinaE-mail: yangk@tsinghua.edu.cn**Keywords:** southern Tibetan Plateau, Asian monsoon, decadal variability, precipitation change

Abstract

The Tibetan Plateau (TP), as a whole, has undergone a moistening process since the late 1990s. However, the southern Tibetan Plateau (STP) is an exception, where summer monsoon precipitation amount has decreased, and lakes have shrunk. The cause for the precipitation decrease is not clear yet. Here we show that the monsoon (June to September) mean precipitation changes in the STP from 1979 to 2018 features a decadal variation component with a peak of around 10 years that is superposed on an upward 'trend' from 1979 to 1998 and a downward 'trend' afterward. We find that the decadal variation of the STP precipitation is associated with a large-scale dipolar sea surface temperature (SST) pattern between the equatorial central Pacific and the Indo-Pacific warm pool. A wet STP corresponds to negative SST anomaly in the equatorial central Pacific and positive SST anomaly in the Indo-Pacific warm pool. This equatorial SST gradient in the western Pacific generates pronounced easterly anomalies and a dipolar rainfall anomaly (i.e. a positive rainfall anomaly over the Maritime Continent and a negative anomaly in the equatorial western and central Pacific). Due to less precipitation over the equatorial western Pacific, the suppressed heat source appears to excite an anomalous anticyclonic band along 15–20° N extending from the Philippine Sea to the Bay of Bengal by emanating westward propagating descending transient Rossby waves. The low-level anticyclonic circulation over the Bay of Bengal further enhances northward moisture transport toward the STP and promote upward motion in the STP through changing local meridional circulation. Besides, the linearized atmospheric general circulation model experiments demonstrate that the dipole heating source can generate a high-pressure zone under the control of anticyclone over the western Pacific, which can extend westward to the Indian monsoon region.

1. Introduction

The Tibetan Plateau (TP) is a critical region for the Asian hydrological cycle because it is the headwater area for the major rivers over Asia (e.g. the Yangtze River, Yellow River, Mekong River, Brahmaputra River, Ganges River, and Indus River). During the past decades, the TP has experienced evident climate changes, e.g. a rising surface air temperature (Wang *et al* 2008, Chen *et al* 2015), an increase in water vapor amount (Lu *et al* 2015), a decrease in solar radiation (Yang *et al* 2012), which have significantly affected

the regional environment (Kang *et al* 2010, Yao *et al* 2019).

The TP boasts the greatest concentration of high-altitude inland lakes in the world. Recent estimates indicate that more than 30 000 lakes with a total area of 51 000 km² are distributed across the TP (Ma *et al* 2011, Zhang *et al* 2019). Some lake basins on the TP contain glaciers, and the glacier melting may contribute to lake mass balance (Zhu *et al* 2010). On the central and western TP, most of the lakes expanded rapidly since the middle of the 1990s, which is mainly attributed to an increase of precipitation

amount (Morrill 2004, Liu *et al* 2010, Lei *et al* 2013, 2014, Zhang *et al* 2017), although accelerating glacier melting can be a great contributor to the lake area variability (Zhu *et al* 2010). However, Yang *et al* (2011) found a decreasing trend from 1984 to 2006 in precipitation from station data in the southern TP (STP), and Gao *et al* (2014) found a similar trend for the period of 1979–2011. This phenomenon was also observed in the nearby central Himalaya (Salerno *et al* 2015). The decrease in precipitation in the STP has led to a significant shrinkage of the lakes since the late 1990s (Lei *et al* 2014, Yang *et al* 2016), making it an exception to the overall expansion of the lakes in the TP. So it is critical to understand the variability of precipitation and its cause for this region. This study aims to explore the conditions that lead to a dry or wet STP during summer monsoon (June–July–August–September (JJAS)) and to understand the physical processes that link the atmosphere–ocean interaction and STP summer monsoon precipitation.

2. Study area and data

The area concerned in this paper is the STP (85–105° E, 26.5–30° N), which covers the central and eastern Himalayas. Some large lakes in the region, such as Yamzho Yumco, Peiku Co, and Puma Yumco, play an important role in shaping the local ecological environment. In this region, the average elevation is more than 5 km, and the terrain is exceptionally complex. Thus, rain gauges are sparsely distributed in this region.

The data used in this study include station rainfall data, gridded rainfall data, and reanalysis data. There are 12 stations in the STP from China Meteorological Administration (CMA), and their locations are shown in figure 1(a). The homogeneity and reliability of CMA data were checked for strict quality control (Chen and Sun 2017). The gridded rainfall data was made through observations and satellite by the Global Precipitation Climatology Project (GPCP), with a resolution of 2.5° latitude by 2.5° longitude (Adler *et al* 2003). The reanalysis data is monthly atmospheric circulation data from ERA-Interim with a resolution of 0.75° (Dee *et al* 2011). All datasets are collected for the 40 year of 1979–2018.

3. Result

3.1. Observed summer monsoon precipitation variability in the STP

Figure 1(b) presents the seasonal variation of precipitation averaged over the STP *in situ* data from 1979 to 2018. The precipitation during JJAS accounts for more than 60% of the annual precipitation, which plays a crucial role in river discharge and downstream water resources. Thus, the JJAS mean precipitation averaged over the 12 stations in the STP is chosen

to represent a monsoon rainfall index of the study region.

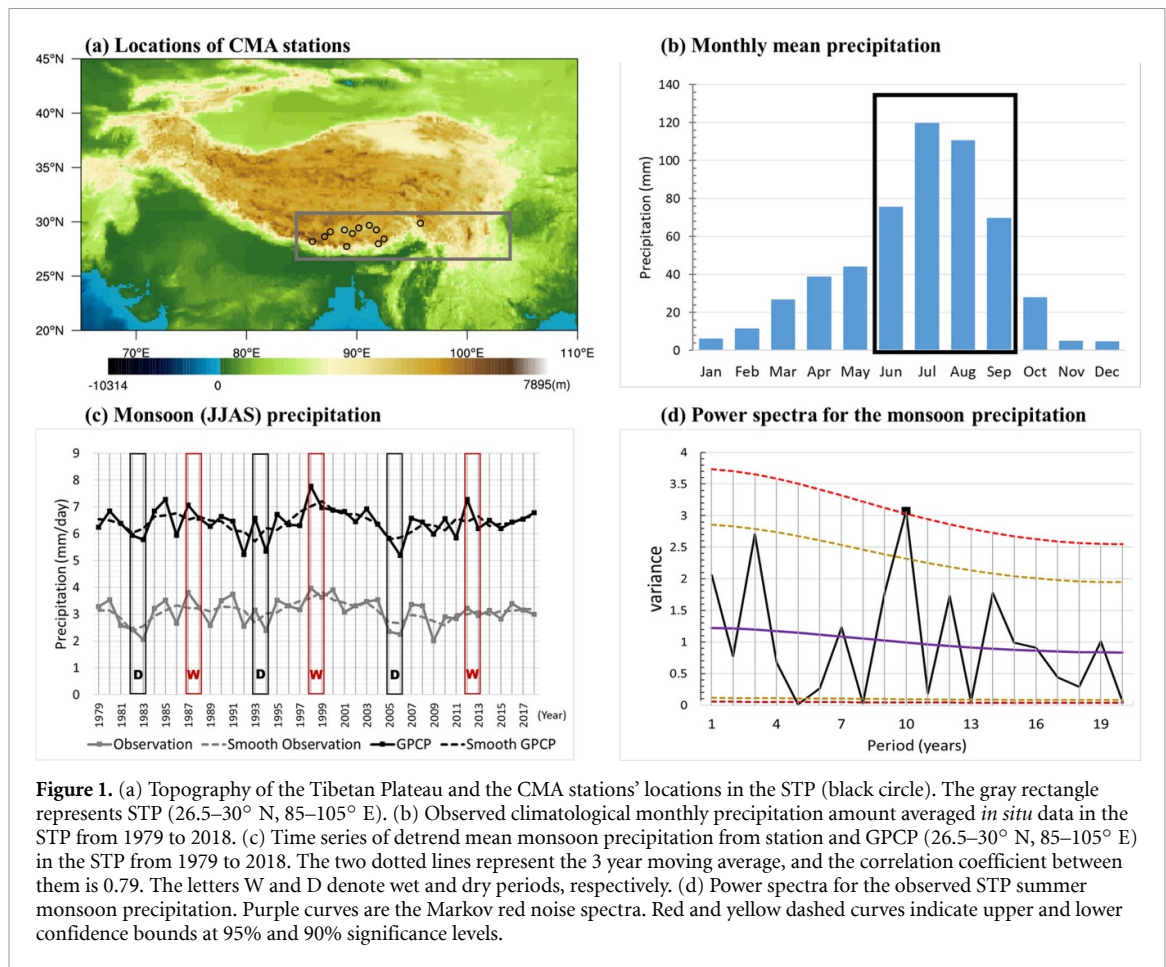
The time series of the STP summer monsoon precipitation (figure 1(c)) shows interannual and decadal fluctuations. Spectral analysis suggests a statistically significant 10 year peak (figure 1(d)). The interannual spectral peak at 3 years is insignificant. The STP summer monsoon rainfall does not link to ENSO significantly with a simultaneous correlation coefficient of 0.17.

To focus on decadal variation, we used a simple 3 year running mean to reduce interannual fluctuations. The 3 year running mean time series suggest that there is no significant trend across the entire 40 year period. Given the homogeneity of the station rain gage data, the conclusion here seems to be credible (Chen and Sun 2017). Thus, the drying trends discussed in the literature (Yang *et al* 2011, Gao *et al* 2014) could be part of the multidecadal variability. Note also that the drying trend in the STP precipitation since 1998 is not a persisting downward trend, and it has been weakened due to a rebound after 2009 with the driest years occurring around 2005–2006. Superposed on the possible multidecadal variation, a decadal variation signal is shown by the spectral analysis (figure 1(d)). From this perspective, the present study focuses on the decadal variation of the STP summer monsoon precipitation based on the 3 year running mean time series.

3.2. Possible mechanisms of the decadal variability of the STP summer monsoon rainfall

We tried to explore the different conditions between the wet and dry STP periods and possible drivers of the decadal variability of the STP summer monsoon rainfall. As shown in figure 1(c), the two dotted lines represent the 3 year moving average from station observations and GPCP precipitation data (26.5–30° N, 85–105° E), respectively, and the correlation coefficient between them is 0.79, which is significant at the 95% confidence level. The significance test has taken into account of the degree of freedom reduction due to 3 year running mean (Livezey and Chen 1983). Considering that there are only 12 observed stations in the STP from 1979 to 2018 and their location is concentrated east of 95° E with limited spatial representation, the GPCP precipitation data is further used to calculate the STP summer monsoon rainfall index and in the analysis below.

In searching for the possible drivers of the decadal variability of the STP summer monsoon rainfall, we select three decadal cycles consisting of three wet and three dry periods from the STP rainfall decadal variation and make a composite analysis. The wet periods are 1987–1988, 1998–1999 and 2012–2013, and the dry periods are 1982–1983, 1993–1994 and 2005–2006. The different meteorological conditions between the wet and dry periods are presented in figure 2. Corresponding to the STP wet periods, there



is a dipolar sea surface temperature (SST) anomaly pattern between the equatorial central and western Pacific and Maritime Continent (MC) with a prominent SST gradient between the two regions. The positive SST anomalies extend from the MC poleward in the western Pacific and the eastern Indian Ocean. In addition, a notable positive anomaly is seen in the southeastern Indian Ocean (IO). The SST gradients between the equatorial central and the MC-southeastern IO generate significant equatorial easterly anomalies at 850 hPa toward the MC (figure 2(a)). The anomalous low-level winds and associated moisture convergence enhances the summer monsoon rainfall over the MC (figure 2(b)). Meanwhile, the equatorial easterly anomalies contribute to the resultant anticyclonic shear vorticity over the equatorial western Pacific, resulting in sinking motion and a large area of dry anomalies there. Thus, a dipolar anomalous rainfall anomaly forms with a positive rainfall anomaly over the MC and a negative anomaly in the equatorial western and central Pacific between 10° S and 10° N (figure 2(b)). The heat source anomalies due to the dipolar rainfall pattern are associated with several anomalous anticyclones over the subtropical western Pacific extending from the Philippine Sea to Indochina Peninsula. The high-pressure zone under the control of anticyclone suppressed convective activity and formed a dry

zone roughly between 10° N and 20° N across South Asia (figure 2(b)). The delicate northwestward tilt of the dry zone may be due to a northward propagation component of the emanated Rossby waves under the eastern vertical shear (Wang and Xie 1996, Xie and Wang 1996). To the south and north of this pronounced dry zone are two bands of enhanced rainfall, the southern one is connected with the enhanced MC rainfall, and the northern one extends from the Himalayas eastward to the Yangtze River Valley. The corresponding STP wetting condition is part of this large-scale triple-band precipitation anomalies. On the regional scale, the southwesterly monsoon is enhanced from the Bay of Bengal and IO to the STP, transporting more moist air toward STP (figure 2(b)). We have further made the composite analysis by using all samples within the positive and negative phases that deviate from the average by greater than 0.1 mm per day in the decadal variation of the STP monsoon precipitation. The results are similar.

The triple-band structure of the precipitation anomalies over South Asia suggests a strong meridional linkage between the anomalous rain bands through meridional overturning circulation. Figure 2(c) presents the composite anomalies (wet periods minus dry periods) of local meridional circulation averaged along the STP longitudes between 85° E and 105° E. It was found that airflows descend

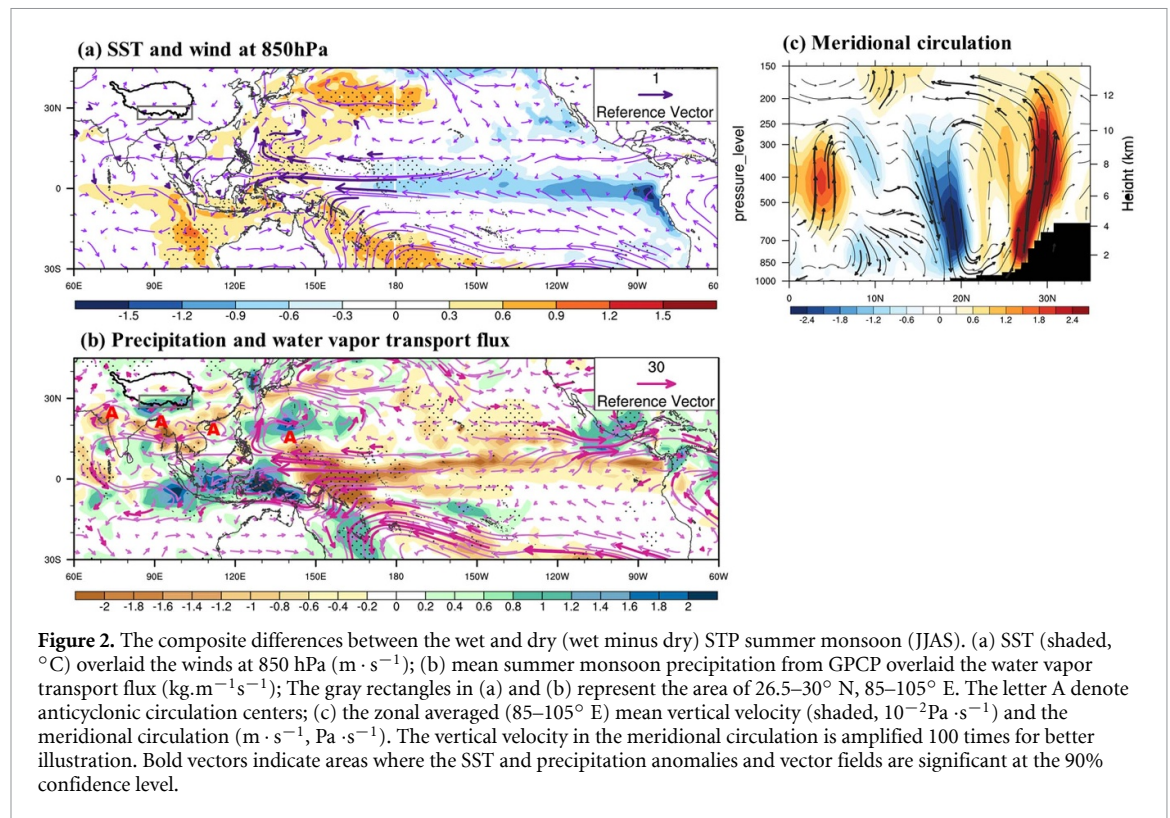


Figure 2. The composite differences between the wet and dry (wet minus dry) STP summer monsoon (JJAS). (a) SST (shaded, °C) overlaid the winds at 850 hPa ($\text{m} \cdot \text{s}^{-1}$); (b) mean summer monsoon precipitation from GPCP overlaid the water vapor transport flux ($\text{kg} \cdot \text{m}^{-1} \cdot \text{s}^{-1}$); The gray rectangles in (a) and (b) represent the area of 26.5–30° N, 85–105° E. The letter A denote anticyclonic circulation centers; (c) the zonal averaged (85–105° E) mean vertical velocity (shaded, $10^{-2} \text{Pa} \cdot \text{s}^{-1}$) and the meridional circulation ($\text{m} \cdot \text{s}^{-1}$, $\text{Pa} \cdot \text{s}^{-1}$). The vertical velocity in the meridional circulation is amplified 100 times for better illustration. Bold vectors indicate areas where the SST and precipitation anomalies and vector fields are significant at the 90% confidence level.

around 20° N and ascend along 25–30° N during the wet STP. The vertical velocity shows strong ascent anomalies over the STP driven by strong sinking motion over the Bay of Bengal and low-level northward flows. Both the meridional sector and horizontal map indicates positive water vapor anomalies over the STP. Therefore, during the cold equatorial central and western Pacific, moisture convergence and water vapor transport over the STP are enhanced, resulting in more precipitation. Furthermore, the dry periods show the opposite conditions to that mentioned above.

We argue that the SST gradient-induced dipolar rainfall anomaly plays a critical role in producing the decadal signals seen in STP and South Asian monsoon precipitation. The positive atmosphere-ocean feedback allows this anomaly to be maintained during JJAS. When the SST in the equatorial central Pacific is in cold condition, the equatorial SST gradients-induced anomalous easterlies over the western Pacific promote the formation of anticyclonic shear vorticity over the Philippine Sea. In turn, the anomalous anticyclonic winds can induce cold SST anomalies and suppress convective precipitation to the south of the anticyclonic center through increased northeast winds which can enhance evaporation cooling in the presence of favorable monsoon background flows and bring dry and cold air (air with low moist static energy) from the north. Thus, the positive atmosphere-ocean feedback allows the rainfall anomalies associated with SST anomalies being maintained in this region during JJAS (Wang et al 2000). The resultant ocean cooling and anomalous

water vapor divergence would enhance descending Rossby waves in their decaying westward journey (Wang et al 2013). Rossby waves continued to extend westward, triggering a series of anomalous anticyclone circulation around 15° N and suppressing precipitation (figure 2(b)). The strong sinking anomaly around 20° N promotes convective motion in the STP through meridional circulation, forming a wet zone. Similarly, the positive feedback between the atmosphere and underlying IO may maintain the warm and wet conditions over the southeast Indian Ocean and the southern MC, as discussed in Wang et al (2003).

3.3. Verification of the theory using general circulation model experiments

To elucidate the physical mechanisms in section 3.2, we performed a numerical experiment with a linearized atmospheric general circulation model (AGCM) (Watanabe and Kimoto 2000, Wang et al 2008). As shown in figure 3(a), we imposed a positive heating source over the MC (5° S–5° N, 90–130° E) with the maximum heating rate ($\sigma = 0.45$) being 1 K per day. The specified negative heating source was set over the western North Pacific (WNP) (5–15° N, 130–155° E), and the minimum heating rate ($\sigma = 0.45$) is -1 K per day. The model was linearized about the climatological July–August mean states. Figure 3(b) indicates the mean flows from 15 to 25 d after the start of the forcing experiment. The results show a high-pressure zone associated with anomalous anticyclone circulation at 850 hPa over the subtropical WNP and southeast China. The resultant ocean cooling over

the WNP would generate descending Rossby waves in their westward journey, extending to Indian monsoon region and enhancing the high-pressure zone over South Asia along 10–20° N. To the south of the TP, the low-level anticyclonic circulation over the Bay of Bengal enhances northward moisture transport toward the STP and promote upward motion in the STP through changing local meridional circulation. Xiang and Wang (2013) made a similar experiment that the positive heat source was placed over the region of 0–20° N, 120–160° E, and the results show an elongated cyclone zone stretching from the Philippine Sea to the Bay of Bengal. When cooling is specified in that region, the response would be consistent with our results in section 3.2. It is worth mentioning that the mean summer monsoon wind field is very important for the westward transmission of Rossby waves. In the absence of background mean flow and boundary moisture feedback, the atmospheric wind response is weak (Wang and Xie 1996, Xiang and Wang 2013). In addition, the power spectrum of the time series of the dipole pattern show a 9 year oscillation, which is similar to a cycle of around 10 years (figure omitted)

4. Summary and discussion

It was reported that the TP had undergone an overall moistening trend in recent decades, but the STP is an exception, where precipitation decreased since the middle of the 1990s, causing glacier retreat (Yao *et al* 2012) and lake shrinkage (Lei *et al* 2014). This study finds an insignificant trend across the entire 40 year period from 1979 to 2018. The trends in the recent two decades discussed in the literature could be part of the multidecadal variability, which show an increasing epoch from 1979 to 1998 and the decreasing period from 1999 to 2018 (figure 1(c)). The decreasing STP precipitation since the late 1990s has been weakened due to a rebound after 2009. Furthermore, we find the STP precipitation varies on the decadal time scale with a statistically significant peak of about 10 years during these 40 years (figure 1(d)). Analysis of the SST and large-scale circulation associated with the decadal variability reveals that the increased STP precipitation is part of the large scale Asian precipitation anomaly pattern that is characterized by a dry zone around 10–20° N (extending from the Philippine Sea to the central India) and a wet zone to its south (Maritime continent and the equatorial Indian Ocean), and another wet zone to its north (the STP) (figure 2(b)). We also find that this triple precipitation anomaly bands are originated from a dipolar precipitation anomaly over the warm pool with enhanced convection over the MC and suppressed rainfall over the equatorial western Pacific. The precipitation dipole is induced by the SST gradients between the cool central Pacific and a warm ocean centered around the MC (figure 2(a)).

The processes by which the decadal SST dipole drives the STP precipitation variation are suggested below along with the schematic diagram (figure 4).

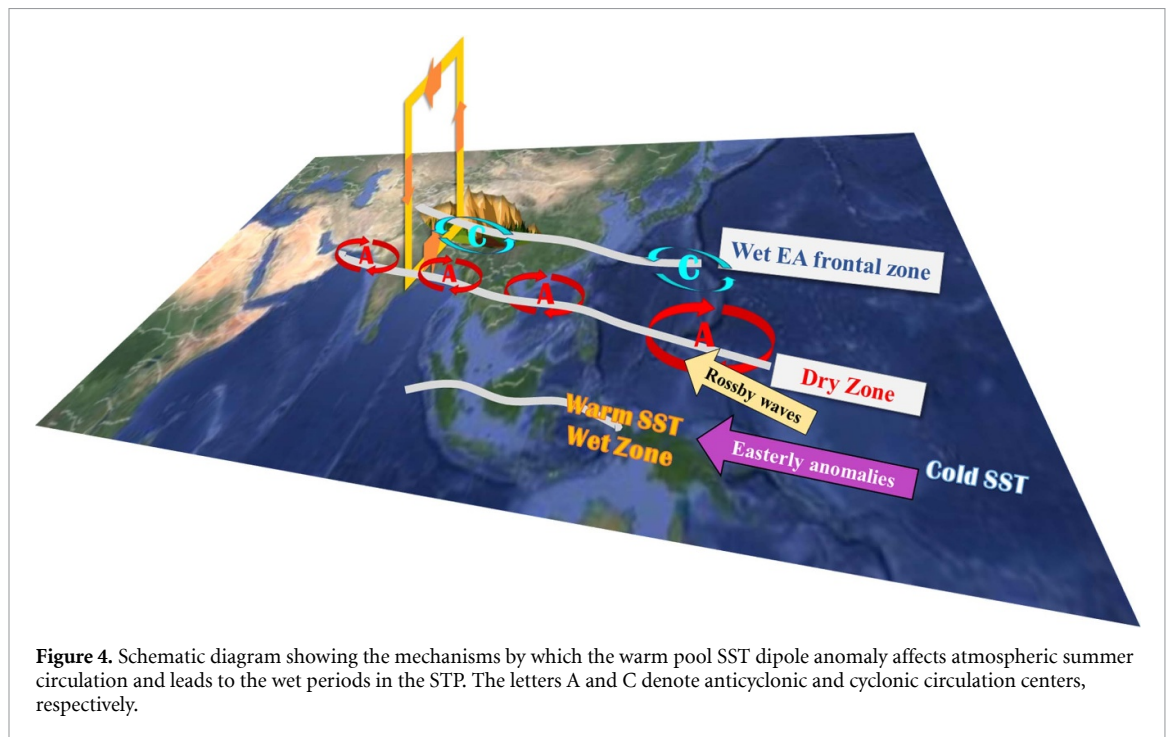
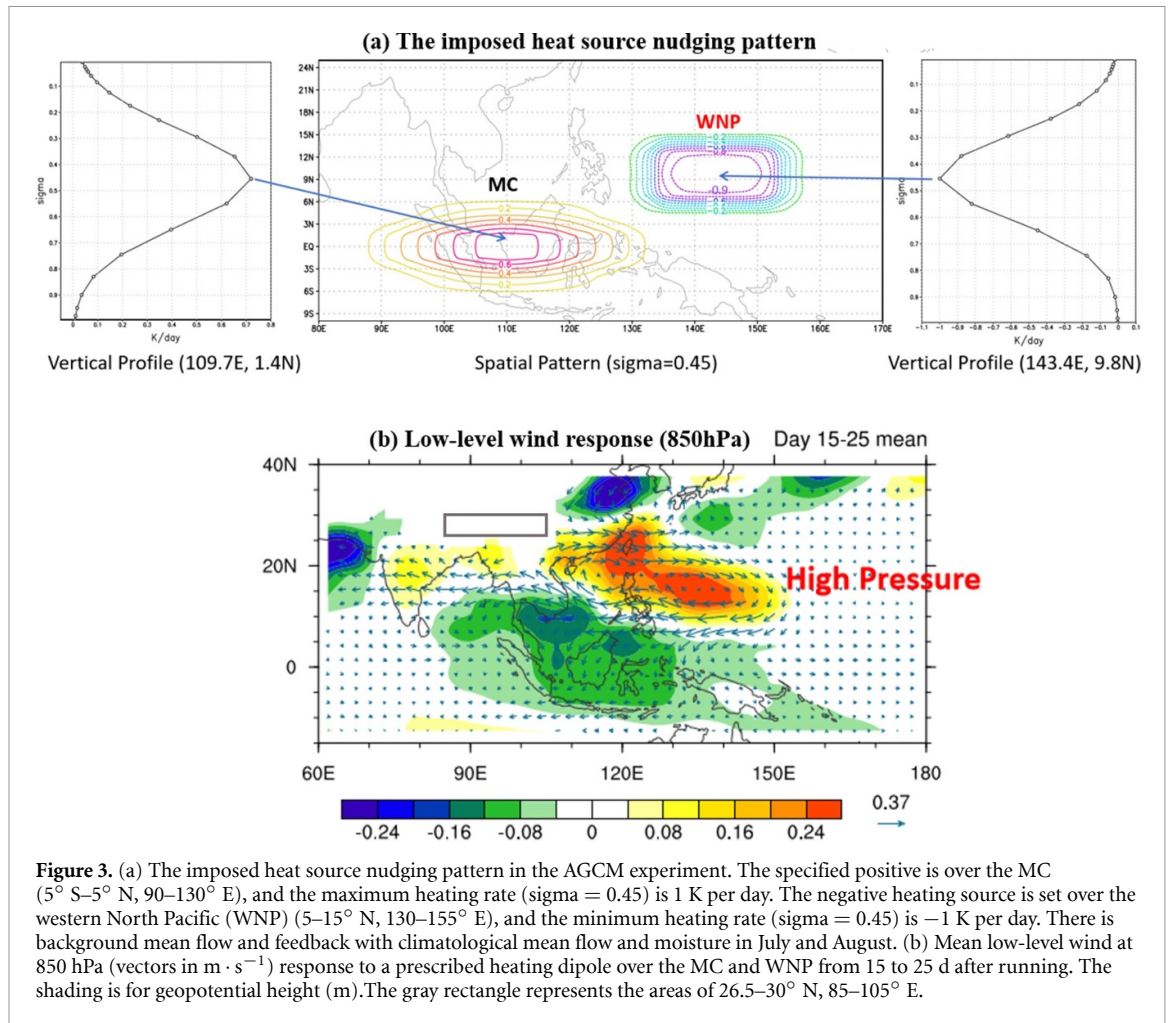
First, the gradient between the lower SST in the equatorial Pacific near the dateline and the higher SST in the MC generates equatorial easterly anomalies, and the meridional shear vorticity generates an anomalous low-level anticyclone over the Philippine Sea, which is essentially a Rossby wave response to the suppressed rainfall in the equatorial western Pacific. The suppressed heating over the Philippine Sea further generates descending transient Rossby waves that propagate westward and form a water vapor divergence band in their westward journey, suppressing convection and forming a dry zone around 10–20° N extending from the Philippine Sea to the Bay of Bengal and central India. Through the local meridional circulation, the airflows descend around 15–20° N over the Bay of Bengal and ascend along 25–30° N, increasing upward motion and precipitation over the STP (figure 2(c)). Meanwhile, the southwesterly monsoon associated with the Bay of Bengal anticyclone enhanced the northward transport of more moist air from the Bay of Bengal and IO to the STP.

Second, the positive atmosphere-ocean feedback allows the dipolar rainfall pattern associated the SST anomalies in the western Pacific-eastern Indian Ocean warm pool to be maintained in this region during the whole monsoon season. On the one hand, the dipolar rainfall anomalies-induced atmospheric heating can generate off-equatorial atmospheric Rossby waves; on the other hand, the Rossby wave-induced low-level circulation anomalies superposed on the seasonal mean circulation can, in turn, strengthen the original dipolar SST anomalies and further increase rainfall in the region. These positive thermodynamic feedback processes can maintain both the negative SST anomalies over the western Pacific and the positive SST anomalies in the equatorial southeastern Indian Ocean, as illustrated by Wang *et al* (2003).

We further did a linearized AGCM experiment to support the mechanism. The simulation results show that the dipole heating source can generate the high-pressure zone under the control of anticyclone over the western Pacific, extending to Indian monsoon region.

In addition to the mechanism proposed above, other factors may affect STP precipitation, such as atmospheric aerosols. The TP is close to northern India with severe anthropogenic aerosol emissions. Related studies indicate that the polluted aerosols can even pass through the Himalayan mountain and reach STP, affecting the formation and development of clouds and precipitation (Lüthi *et al* 2015, Dong *et al* 2016). However, it is still unclear about the impact of atmospheric aerosols on the STP due to the limited observations and research (Zhao *et al* 2020).

The 40 year data is too short to firmly conclude the existence of the decadal oscillation found over the



STP and South Asia. However, Sontakke *et al* (2008) examined the long record of observational rainfall data since 1800 and found 11 year, 23 year, and 65 year

peaks in the Indian summer monsoon precipitation. In a recent study, Shi *et al* (2019) examined the reconstructed Asian precipitation data from 1470 to 2013.

They found that the Asian summer precipitation has significant spectral peaks on decadal (8–10 years) and multidecadal (50–60 years) time scales mainly over the MC and the monsoon region. The present finding appears to be consistent with the findings above with long records. Shi *et al* (2019) suggested that during the industrial period, the enhanced Asian summer monsoon rainfall on the decadal time scale is associated with a mega-La Niña like SST pattern over the Pacific, which seems to be consistent with our finding here. However, the precise cause of the decadal variation in Asian summer monsoon remains elusive. We speculate that besides the internal variability of the coupled atmosphere-ocean-land system in the Pacific-Asian region, the decadal forcing in solar irradiance could contribute to the decadal variability of the Asian summer monsoon. The 11 year solar cycle has been shown to have a significant impact on the EA summer monsoon rainfall and EA winter temperature (Jin *et al* 2019). The potential contribution from both the internal variability and external forcing deserves further exploration. The decadal STP precipitation variation is part of the Asian summer monsoon variability and possibly linked to the Pacific quasi-decadal oscillation (Wang *et al* 2014). The fundamental cause of the decadal variability of the Asian monsoon-Indo-Pacific warm pool system, which may be associated with ENSO low-frequency variations, calls for further study.

Acknowledgments

This work was supported by the Second Tibetan Plateau Scientific Expedition and Research Program (Grant No. 2019QZKK0206), the Strategic Priority Research Program of Chinese Academy of Sciences, Grant No. XDA2006010201) and Tsinghua tutor research fund. B W acknowledges the support from NSF/Climate Dynamics Award #AGS-1540783. This is the ESMC publication number 333.


Data availability statement

The data that support the findings of this study are available upon reasonable request from the authors.

ORCID iDs

Siyu Yue  <https://orcid.org/0000-0002-4604-5728>

Kun Yang  <https://orcid.org/0000-0002-0809-2371>

Zhiling Xie  <https://orcid.org/0000-0002-9457-8465>

Hui Lu  <https://orcid.org/0000-0003-1640-239X>

References

- Adler R F *et al* 2003 The version-2 global precipitation climatology project (GPCP) monthly precipitation analysis (1979–present) *J. Hydrometeorol.* **4** 1147–67

- Chen D *et al* 2015 Assessment of past, present and future environmental changes on the Tibetan Plateau *Chin. Sci. Bull.* **60** 3025–35
- Chen H and Sun J 2017 Contribution of human influence to increased daily precipitation extremes over China *Geophys. Res. Lett.* **44** 2436–44
- Dee D P *et al* 2011 The ERA-Interim reanalysis: configuration and performance of the data assimilation system *Q. J. R. Meteorol. Soc.* **137** 553–97
- Dong W *et al* 2016 Summer rainfall over the southwestern Tibetan Plateau controlled by deep convection over the Indian subcontinent *Nat. Commun.* **7** 1–9
- Gao Y, Cuo L and Zhang Y 2014 Changes in moisture flux over the Tibetan Plateau during 1979–2011 and possible mechanisms *J. Clim.* **27** 1876–93
- Jin C, Wang B, Liu J, Ning L and Yan M 2019 Decadal variability of northern Asian winter monsoon shaped by the 11 year solar cycle *Clim. Dyn.* **53** 6559–68
- Kang S, Xu Y, You Q, Flugel W, Pepin N and Yao T 2010 Review of climate and cryospheric change in the Tibetan Plateau *Environ. Res. Lett.* **5** 15101
- Lei Y, Yang K, Wang B, Sheng Y, Bird B W, Zhang G and Tian L 2014 Response of inland lake dynamics over the Tibetan Plateau to climate change *Clim. Change* **125** 281–90
- Lei Y, Yao T, Bird B W, Yang K, Zhai J and Sheng Y 2013 Coherent lake growth on the central Tibetan Plateau since the 1970s: characterization and attribution *J. Hydrol.* **483** 61–67
- Liu J, Kang S, Gong T and Lu A 2010 Growth of a high-elevation large inland lake, associated with climate change and permafrost degradation in Tibet *Hydrol. Earth Syst. Sci.* **14** 481–9
- Livezey R E and Chen W Y 1983 Statistical field significance and its determination by Monte Carlo techniques *Mon. Weather Rev.* **111** 46–59
- Lu N, Trenberth K E, Qin J, Yang K and Yao L 2015 Detecting long-term trends in precipitable water over the Tibetan Plateau by synthesis of station and MODIS observations *J. Clim.* **28** 1707–22
- Lüthi Z L, Škerlak B, Kim S W, Lauer A, Mues A, Rupakheti M and Kang S 2015 Atmospheric brown clouds reach the Tibetan Plateau by crossing the Himalayas *Atmos. Chem. Phys.* **15** 6007–21
- Ma R *et al* 2011 China's lakes at present: number, area and spatial distribution *Sci. China Earth Sci.* **54** 283–9
- Morrill C 2004 The influence of Asian summer monsoon variability on the water balance of a Tibetan lake *J. Paleolimnol.* **32** 273–86
- Salerno F *et al* 2015 Weak precipitation, warm winters and springs impact glaciers of south slopes of Mt. Everest (central Himalaya) in the last 2 decades (1994–2013) *Cryosphere* **9** 1229–47
- Shi H, Wang B, Liu J and Liu F 2019 Decadal–multidecadal variations of Asian summer rainfall from the little ice age to the present *J. Clim.* **32** 7663–74
- Sontakke N, Singh N and Singh H 2008 Instrumental period rainfall series of the Indian region (AD 1813–2005): revised reconstruction, update and analysis *Holocene* **18** 1055–66
- Wang B, Bao Q, Hoskins B, Wu G and Liu Y 2008 Tibetan Plateau warming and precipitation changes in East Asia *Geophys. Res. Lett.* **35** 14
- Wang B, Wu R and Fu X 2000 Pacific-East Asian teleconnection how does ENSO affect East Asian climate? *J. Clim.* **13** 1517–36
- Wang B, Wu R and Li T 2003 Atmosphere–warm ocean interaction and its impacts on Asian–Australian monsoon variation *J. Clim.* **16** 1195–211
- Wang B, Xiang B and Lee J Y 2013 Subtropical high predictability establishes a promising way for monsoon and tropical storm predictions *Proc. Natl Acad. Sci. USA* **110** 2718–22

- Wang B and Xie X 1996 Low-frequency equatorial waves in vertically sheared zonal flow. Part I: stable waves *J. Atmos. Sci.* **53** 449–67
- Wang S, Hakala K, Gillies R R and Capehart W J 2014 The Pacific quasi-decadal oscillation (QDO) an important precursor toward anticipating major flood events in the Missouri River Basin? *Geophys. Res. Lett.* **41** 991–7
- Watanabe M and Kimoto M 2000 Atmosphere-ocean thermal coupling in the North Atlantic: a positive feedback *Q. J. R. Meteorol. Soc.* **126** 3343–69
- Xiang B and Wang B 2013 Mechanisms for the advanced Asian summer monsoon onset since the mid-to-late 1990s *J. Clim.* **26** 1993–2009
- Xie X and Wang B 1996 Low-frequency equatorial waves in vertically sheared zonal flow. Part II: unstable waves *J. Atmos. Sci.* **53** 3589–605
- Yang K, Ding B, Qin J, Tang W, Lu N and Lin C 2012 Can aerosol loading explain the solar dimming over the Tibetan Plateau? *Geophys. Res. Lett.* **39** 20
- Yang K, Ye B, Zhou D, Wu B, Foken T, Qin J and Zhou Z 2011 Response of hydrological cycle to recent climate changes in the Tibetan Plateau *Clim. Change* **109** 517–34
- Yang R, Zhu L, Wang J, Ju J, Ma Q, Turner F and Guo Y 2016 Spatiotemporal variations in volume of closed lakes on the Tibetan Plateau and their climatic responses from 1976 to 2013 *Clim. Change* **140** 621–33
- Yao T et al 2012 Different glacier status with atmospheric circulations in Tibetan Plateau and surroundings *Nat. Clim. Change* **2** 663–7
- Yao T et al 2019 Recent third pole's rapid warming accompanies cryospheric melt and water cycle intensification and interactions between monsoon and environment: multidisciplinary approach with observations, modeling, and analysis *Bull. Am. Meteorol. Soc.* **100** 423–44
- Zhang G, Li J and Zheng G 2017 Lake-area mapping in the Tibetan Plateau: an evaluation of data and methods *Int. J. Remote Sens.* **38** 742–72
- Zhang G, Luo W, Chen W and Zheng G 2019 A robust but variable lake expansion on the Tibetan Plateau *Sci. Bull.* **64** 1306–9
- Zhao C, Yang Y, Fan H, Huang J, Fu Y, Zhang X, Kang S, Cong Z, Letu H and Menenti M 2020 Aerosol characteristics and impacts on weather and climate over the Tibetan Plateau *Natl Sci. Rev.* **7** 492–5
- Zhu L, Xie M and Wu Y 2010 Quantitative analysis of lake area variations and the influence factors from 1971 to 2004 in the Nam Co basin of the Tibetan Plateau *Chin. Sci. Bull.* **55** 1294–303